Family with sequence similarity 83, member B is a predictor of poor prognosis and a potential therapeutic target for lung adenocarcinoma expressing wild-type *epidermal growth factor receptor*

TAKUMI YAMAURA[1], JUNJI EZAKI[2], NAOYUKI OKABE[1], HIRONORI TAKAGI[1], YUKI OZAKI[1], TAKUYA INOUE[1], YUZURU WATANABE[1], MITSURO FUKUHARA[1], SATOSHI MUTO[1], YUKI MATSUMURA[1], TAKEO HASEGAWA[1], MIKA HOSHINO[1], JUN OSUGI[1], YUTAKA SHIO[1], SATOSHI WAGURI[3], HIROSUMI TAMURA[2], JUN-ICHI IMAI[2], EMI ITO[2], YUKA YANAGISAWA[2], REIKO HONMA[4], SHINYA WATANABE[2], and HIROYUKI SUZUKI[1]

[1] Department of Chest Surgery, Fukushima Medical University School of Medicine, Fukushima 960-1295, Japan

[2] Medical-Industrial Translational Research Center, Fukushima Medical University

School of Medicine, Fukushima 960-1295, Japan

[3] Department of Anatomy and Histology, Fukushima Medical University School of Medicine 960-1295, Fukushima, Japan

[4] Nippon Gene Co., Ltd., Tokyo 101-0054, Japan

Corresponding author: Hiroyuki Suzuki

Department of Chest Surgery, Fukushima Medical University School of Medicine, 1, Hikarigaoka, Fukushima, 960-1295, Japan

E-mail: hiro@fmu.ac.jp

Keywords: *family with sequence similarity 83, member B*, lung adenocarcinoma, wild-type epidermal growth factor receptor, poor prognosis, biomarker

Running title: YAMAURA et al: FAM83B IS UPREGULATED IN WILD-TYPE

Abstract (241/150-300 words)

Lung adenocarcinoma (ADC) patients with tumors that harbor no targetable driver gene mutation, such as epidermal growth factor receptor gene (EGFR) mutations, have unfavorable prognosis, and novel therapeutic targets are needed. We have reported that *family with sequence similarity 83, member B* (*FAM83B*) is a biomarker for squamous cell lung cancer. FAM83B has recently been shown to play an important role in the EGFR signaling pathway. In this study, we investigated the molecular and clinical impact of FAM83B in lung ADC. Matched tumor and adjacent normal tissue samples were obtained from 216 patients who underwent complete lung resection for primary lung ADC and were examined for *FAM83B* expression using cDNA microarray analysis. The relationships between *FAM83B* expression and clinicopathological parameters, including patient survival, were examined. *FAM83B* was highly expressed in tumors

from males, smokers, and in tumors with wild-type *EGFR*. Multivariate analyses further confirmed that wild-type *EGFR* tumors were significantly positively correlated with *FAM83B* expression. In survival analysis, *FAM83B* expression correlated with poor outcome in both disease-free survival and overall survival, especially when stratified against tumors with wild-type *EGFR*. Furthermore, *FAM83B* knockdown was performed to investigate its phenotypic effect on lung ADC cell lines. Gene silencing by *FAM83B* RNA interference caused growth suppression of HLC-1 and H1975 lung ADC cell lines. *FAM83B* may be involved in lung ADC tumor proliferation and can be a predictor of poor survival. *FAM83B* is also a potential novel therapeutic target for ADC with wild-type *EGFR*.

Introduction

Cancers are among the leading causes of mortality worldwide, with 8.2 million cancer-related deaths in 2014. Among different cancers, lung cancer has the highest

mortality rate with 1.59 million deaths; this is more than twice the number of hepatocellular carcinoma deaths, which is the second most fatal form of cancer (1). Lung cancer patients have poor prognosis and at initial hospital visit are often diagnosed at an advanced stage, beyond the possibility of surgical intervention (2).

Cytotoxic chemotherapeutic agents are usually administered for advanced lung cancer therapy and are chosen according to histological subtype. Recently, molecular targeted agents and immune checkpoint inhibitors have been developed and have been in clinical use since the 2000s (3). In non-small cell lung cancer, including adenocarcinoma (ADC), which represents 40% of all lung cancers, several types of driver gene mutation that promote oncogenic transformation and tumor growth by aberrant activation of proliferation signaling pathways have been identified (4). These driver genes are proposed as novel candidates for molecular targeted therapy. Epidermal growth factor receptor (EGFR) activating mutations lead to auto-phosphorylation and

promote EGFR/KRAS/MEK/ERK signaling (5). Aberrant anaplastic lymphoma kinase (ALK) protein, produced by an ALK fusion gene, drives MEK/ERK and PI3K/Akt pathways (6). EGFR-tyrosine kinase inhibitor (TKI) and an ALK inhibitor against the above two aberrant signals prevent tumor progression with a high response rate of 56.0%–70.0%, while cytotoxic chemotherapy or immune checkpoint inhibition are successful only in19.0%–34.1% of cases (7-11). Thus, these precision medicines based on genetic or molecular features of lung ADC can provide therapy with a high response rate and fewer adverse effects (7-11). However, 29.2%–40.0% of lung ADC patients have no targetable genetic features (4, 12, 13). There is an urgent need to discover novel biomarkers and therapeutic targets, and studies are ongoing to establish targeted therapy for rare driver gene mutations of malignancy (4).

We have identified and reported *family with sequence similarity 83, member B* (*FAM83B*) as a novel diagnostic and prognostic marker for lung squamous cell cancer

(SqCC) (14). Comprehensive gene expression analysis using cDNA microarray analysis and immunohistochemistry showed lung SqCC expressed higher levels of *FAM83B* compared with lung adenocarcinoma or adjacent normal lung tissue, and correlated with patient prognosis (14). *FAM83B* is also overexpressed in several other types of cancer, such as breast, ovary, bladder, and lung, and is associated with tumor proliferation (15). Additionally, induction of *FAM83B* in human mammary epithelial cells resulted in neoplastic growth by increasing mitogen-activated protein kinase (MAPK) signaling, while induction in human breast cancer cell lines resulted in TKI resistance (15). Aberrant EGFR signals and downstream signaling play an important role in targeted therapy for lung ADC; therefore, we assumed that *FAM83B* also correlates with tumor oncogenesis and growth in lung ADC. Here, we show an association between *FAM83B* expression in lung ADC and demographics and clinicopathological features.

Materials and methods

Ethics statement. This study was conducted with approval of the Ethics Committee of Fukushima Medical University (approval no. 2775). The participants' human rights and welfare were defended in accordance with the Declaration of Helsinki. Written informed consent was obtained from all participants.

Case selection. We identified 216 patients who underwent lung resection at Fukushima Medical University between January 2008 and June 2015 and who were pathologically diagnosed as primary lung ADC. *FAM83B* mRNA levels were determined in matched lung tumor and adjacent normal lung tissue and compared with clinical features and prognosis. The data collected were; age at surgery, sex, smoking history, presence of activating *EGFR* mutation in the tumor, histological ADC subtype, tumor size, lymph node metastasis, distant metastasis, pleural invasion, lymphovascular invasion, vascular invasion, date of surgery, date of recurrence, last confirmed survival date, and date of death. Disease-free survival (DFS) was defined as the time from surgery to the first

recurrence or death. Overall survival (OS) was defined as the time from surgery to death. To ensure a sufficient observation period, prognostic analyses were performed for patients who underwent complete resection up to December 2013, and who were followed up for 5 years. Patients who had an additional advanced malignant history within 5 years before lung resection, died of postoperative complications, or who were followed up for less than 12 months were excluded. In total, 126 patients were analyzed.

Comprehensive gene expression analysis. Matched tumor and adjacent normal lung tissue samples, 7 mm^3 in size, were excised from surgical specimens and frozen in liquid nitrogen. Frozen samples were processed for total RNA extraction using ISOGEN (Nippon Gene, Tokyo, Japan). As a control, common reference RNA was prepared by mixing equal amounts of total RNA extracted from 22 human cell lines to reduce cell type-specific expression bias (16). Synthetic 80mer polynucleotide probes representing 14,400 human transcripts (MicroDiagnostic, Tokyo, Japan) were arrayed using a custom

arrayer. Labeled cDNA was synthesized from 5 μg of sample RNA using SuperScript II (Thermo Fisher Scientific, Waltham, MA, USA) and Cyanine 5-dUTP (Perkin-Elmer, Waltham, MA, USA), while Cyanine 3-dUTP (Perkin-Elmer)-labeled cDNA was synthesized from 5 μg of human common reference RNA. Hybridization was performed using a Labeling and Hybridization kit (Microdiagnostic). Signals were measured using a GenePix 4000B Scanner (Axon instruments, Union city, CA, USA), and then processed into primary expression ratios (ratio of Cyanine-5 intensity of each sample to the Cyanine-3 intensity of human common reference RNA). Each ratio was normalized by multiplication with normalization factors using GenePix Pro 3.0 software (Axon instruments). The primary expression ratios were converted into $\log_2$ fold changes (designated log ratios). An expression ratio of 1 (i.e., log ratio of 0) was assigned to spots that exhibited fluorescence intensities under detection limits, and we included these in the calculation of signal averages. Data were processed using Microsoft Excel

software (Microsoft, Bellevue, WA, USA) and the MDI gene expression analysis software package (MicroDiagnostic). mRNA expression data related to *FAM83B* were extracted for this study.

Preparation of cell lines. HLC-1 cells were purchased from Riken Cell Bank (Saitama, Japan). NCI-H2347, NCI-H1975 and MCF-7 cells were purchased from American Type Culture Collection (Manassas, VA, USA). HLC-1 cells were grown in Ham's F12 medium (087-08335, Wako pure chemical industries, Osaka, Japan). NCI-H2347 and NCI-H1975 cells were grown in RPMI-1640 medium (R8758, Sigma Aldrich, St. Louis, MO, USA), MCF-7 cells were grown in DMEM medium (Wako pure chemical industries). All media contained 10% fetal bovine serum (Nichirei Biosciences, Tokyo, Japan) and 1% penicillin-streptomycin (Sigma-Aldrich). Cells were cultured at 37°C in a humidified atmosphere of 5% CO_2.

siRNA preparation. siRNAs against *FAM83B* were purchased (Hs_FAM83B_8 and

Hs_FAM83B_9 FlexiTube siRNA, Qiagen, Hilden, Germany). Sequences of siRNAs were: Hs_FAM83B_8 (siRNA-8): 5′-CAGGAACGAGTTTCAGACTTT-3′, and Hs_FAM83B_9 (siRNA-9): 5′-TCCCGTTATTTGACAACTCAA-3′.

As a negative control, AllStars negative control siRNA (Qiagen) was used. As a positive control, AllStars Hs Cell Death siRNA (Qiagen) was used.

siRNA transfection efficiency assay. For 96-well siRNA transfections, 0.3 μL of Lipofectamine RNAiMAX (Thermo Fisher Scientific) in 10 μL of serum-free Opti-MEM (Thermo Fisher scientific) was added to preplated siRNAs in each well and incubated for 5 minutes at room temperature. MCF7, HLC-1, H2347, or H1975 cells were added at 1.0×10^4 to each well. After incubation for 72 hours, 10 μL of Cell Counting Kit-8 (Dojindo laboratories, Kumamoto, Japan) was added and absorbance at 450 nm measured 4 hours later using a Multiskan GO (Thermo Fisher scientific) (**Figure 4A-D**). Each test was replicated three times.

RNA interference and cell proliferation assay. According to a transfection efficiency test (**Figure 4**), RNA interference experiments (RNAi) were performed using siRNA-9. siRNA-9 (final concentration of 2.5 nM) and 7.5-μL Lipofectamine RNAiMAX were mixed in 100 μL of serum-free Opti-MEM in a microcentrifuge tube, then added within 20 minutes to cells in 6-well plates. RNAi was performed using 1×10^5 cells/well for HLC-1, and 5×10^4 cells/well for H1975 and replicated three times. To determine the silencing effects of siRNA against *FAM83B*, cell numbers were counted after transfection using Clone select imager (Molecular devices Japan, Tokyo, Japan).

Quantitative real time-polymerase chain reaction (qRT-PCR). Total RNA was isolated from cell lines using TRIzol reagent (Thermo Fisher Scientific) and a PureLink RNA Mini Kit (Thermo Fisher Scientific) according to the manufacturers' instructions. RNA quantity was assessed using a Nanodrop UV-Vis Spectrophotometer (Thermo Fisher Scientific), and samples with a 260/280 nm absorbance ratio of 1.8 or larger were

adopted as eligible for RT-PCR. Relative mRNA expression was determined by RT-PCR. One-step qRT-PCR using a Taqman RNA-to-C_T 1-Step Kit (Thermo Fisher Scientific) was performed according to the manufacturer's instructions. To detect *FAM83B* mRNA, Taqman gene expression assays (Hs00289694_m1, Thermo Fisher Scientific) were used. As an endogenous control, *glyceraldehyde-3-phosphate dehydrogenase* (*GAPDH*, Hs02758991_g1, Thermo Fisher Scientific) was used. Forty cycles of amplification were performed for each triplicated sample. The ΔΔCq method was applied for quantitative evaluation (17). Cycle threshold (Cq) values were calculated by Step One Plus software version 2.3 (Thermo Fisher Scientific). ΔCq was defined as the difference between *FAM83B* Cq and *GAPDH* Cq, and ΔΔCq was defined as the ratio to the endogenous control sample. Signals undetected after 40 cycles were considered to have an expression of zero.

SDS-PAGE. Cell lysates were prepared by homogenization of cells in RIPA lysis buffer

(SC-24948, Santa Cruz Biotechnology, Dallas, TX, USA), using a Polytron homogenizer (Sonifier SFX250, Emerson Electric Co, St. Louis, MO, USA) at 4°C. After centrifugation at 10,000 x g for five minutes at 4°C, supernatants were mixed with an equal volume of Sample buffer (2× Laemmli Sample Buffer, Biorad, Hercules, CA. USA). 2-mercaptoethanol (Biorad, 200:1) was then added and samples heated for three minutes at 100°C. Five micrograms of each sample were then loaded on a polyacrylamide gel (Supersep ace 5%-20%, Wako pure chemical industries) and electrophoresis was performed to separate proteins (18).

Western Blotting. Proteins were transferred to a polyvinylidene difluoride membrane (Immobilon, Merck Millipore corporation, Darmstadt, Germany) in Towbin transfer buffer (25 mM Tris base, 192 mM glycine, 0.1% SDS, 20% methanol) (19). The membranes were then blocked with 5% skimmed milk in PBS (0.137 M NaCl, 2.6 mM KCl, 1.8 mM KH_2PO_4, 8.1 mM $Na_2HPO_4/12H_2O$) and incubated overnight in primary

antibody solution at 4°C. Anti-FAM83B antibodies (1:1,000, PA5-28548, ThermoFisher scientific, or 1:2,000, HPA031464, Atlas antibodies AB, Stockholm, Sweden) or an anti-GAPDH antibody (1:2,500, no.2118, Cell Signaling Technology, Inc., Danvers, MA, USA) were used as primary antibodies. Membranes were then incubated with secondary antibody (anti-rabbit IgG, Horseradish Peroxidase-Linked species-specific whole antibody (1:20,000, GE Health Care UK Ltd., Amersham, UK). The chemiluminescent signals were captured with the ImageQuant LAS 4000 system (GE Health Care UK Ltd.) using ECL select Western Blotting Detection Reagent (GE Health care UK ltd.) according to the manufacturer's instructions.

Statistical analysis. Statistical analyses were performed using SPSS 21.0 (IBM SPSS, Chicago, Il, USA). The patient cohort was divided into two subgroups according to high or low *FAM83B* expression with the log ratio of zero as the boundary. Patients were divided into two groups according to median age. Tumor (T), Nodes (N), and Metastasis

(M) (TNM) factors of lung cancer were classified according to the Union for International Cancer Control 7th edition. T factor was not adopted but tumor size and pleural invasion were. Continuous variables were compared by two-tailed *t*-tests or one-way ANOVA, and categorical variables were compared by the chi-square test or Fisher's exact test, as appropriate. Multivariate analyses using a binary logistic regression model were performed to evaluate independent predictors of *FAM83B* expression. DFS and OS were estimated using the Kaplan–Meier method, and survival curves were compared using log-rank tests. Variables that were suitable for a Cox proportional hazards univariate model with significance were analyzed by a multivariate model to adjust for potential confounders. P values of less than 0.05 were considered statistically significant.

Results

FAM83B is highly expressed in ADC with wild type-EGFR. This study included 119

male and 97 female patients, with a mean age of 68.5 years (range 26–87 years). Up to 111 (51.4%) were current or former smokers, and 118 (54.6%) had wild-type *EGFR* ADC. *FAM83B* tended to be expressed at higher levels in solid subtypes while lower *FAM83B* expression was observed in lepidic pattern tumors that were less aggressive. Mean tumor size was 2.9 cm (range 0.8–14.0). The clinicopathological characteristics of patients according to *FAM83B* expression in tumor tissue are summarized in **Table I**. Univariate analysis showed that higher *FAM83B* expression correlates with males ($p = 0.007$), smoking history ($p = 0.007$), and wild-type *EGFR* tumors ($p < 0.001$). Multivariate analysis showed wild-type *EGFR* tumors correlate with *FAM83B* expression ($p < 0.001$) (**Table II**).

Correlation between FAM83B expression obtained from cDNA microarray analysis and EGFR mutation in lung ADC. The mean *FAM83B* expression in adjacent normal lung tissue (n = 98), wild-type *EGFR* tumors (n = 118) and mutant *EGFR* tumors (n = 98)

was −0.190, standard deviation (SD) of 0.365, 0.877, SD of 0.689, and −0.231, SD of 0.425, respectively. Multiple comparison of these three groups showed that *FAM83B* expression in wild-type *EGFR* tumors was higher than in adjacent normal lung tissue ($p < 0.001$) or mutant *EGFR* tumors ($p < 0.001$), while there was no significant difference between mutant *EGFR* tumors and adjacent normal lung tissue ($p = 0.852$) (**Figure 1**).

FAM83B is a predictor of poor lung ADC prognosis, especially for ADC with wild-type *EGFR*. The *FAM83B* high expression group showed significantly shorter survival times both in DFS ($p = 0.011$) and OS ($p = 0.001$). Subgroup analysis showed that the *FAM83B* high expression group had shorter DFS and OS with wild-type *EGFR* tumors ($p = 0.017$, $p = 0.008$, **Figure 2**), while no significant difference was found in patients with mutant *EGFR* tumors ($p = 0.746$, $p = 0.588$). Survival analysis using a Cox regression hazard model was then conducted. For DFS, univariate analysis showed that high levels of *FAM83B* expression, male sex, lymph node metastasis, pleural invasion,

lymphovascular invasion, and vascular invasion were involved in poor prognosis. Multivariate analysis identified high levels of *FAM83B* expression and lymph node metastasis as independent poor prognostic factors (**Table III**). In OS, univariate analysis showed high levels of *FAM83B* expression, male sex, wild-type *EGFR* tumors, lymph node metastasis, pleural invasion, lymphovascular invasion, and vascular invasion as poor prognostic factors. Multivariable analysis showed high levels of *FAM83B* expression, pleural invasion, and vascular invasion were independent predictors of poor prognosis (**Table III**).

Involvement of FAM83B in cell proliferation in several types of lung cancer cell line. Cell lines derived from lung adenocarcinoma, including HLC-1, H2347 (both wild-type for *EGFR*) and H1975 (mutant *EGFR*), and a positive control breast cancer cell line, MCF7 (15) were prepared. qRT-PCR showed high levels of *FAM83B* expression in HLC-1 and H2347 cells but scarcely detectable levels in H1975 cells (**Figure 3A**).

Immunoblot analysis showed levels of FAM83B that were consistent with the HLC-1, MCF7, and H1973 qRT-PCR results (**Figure 3B**). In MCF7 cells, *FAM83B* knockdown with siRNA-8 or siRNA-9 caused inhibition of cell proliferation (siRNA-8; $p = 0.393$, siRNA-9; $p = 0.061$ at 6 days after knockdown), with siRNA-9 having the stronger anti-proliferative effect (**Figure 4E-G**); therefore, we performed subsequent knockdown experiments using siRNA-9. siRNA transfection efficacy assays (**Figure 4A-D**) indicated *FAM83B* RNAi should be performed in HLC-1 and H1975 cells. Depletion of *FAM83B* expression and suppression of cell proliferation were confirmed in HLC-1 and even in H1975 cells, which expressed low levels of *FAM83B* (**Figure 3C-H**).

Discussion

In this study, we focused on comprehensive gene expression analysis of tumors from resected lungs of Japanese ADC patients, and we showed that *FAM83B* expression was higher in tumors with wild-type *EGFR* compared with tumors with mutant EGFR, and

that *FAM83B* expression was associated with proliferation in cell lines. Furthermore, *FAM83B* expression was identified as a biomarker of poor prognosis from patient clinical outcomes.

FAM83B expression is elevated relative to normal associated tissues in several types of cancer, such as breast, ovary, cervical, testis, thyroid, bladder, lymphoid and lung (15). In lung cancer, analysis of *FAM83B* expression confirmed that *FAM83B* expression was significantly elevated in tumor specimens relative to normal tissues (15). It was also reported that *FAM83B* mRNA levels were significantly higher in SqCC than in normal lung or ADC (14). It is a novel finding that *FAM83B* is more highly expressed in lung ADCs containing wild-type *EGFR* compared with ADCs carrying mutant *EGFR*. Interestingly, in breast cancer, *FAM83B* is expressed at higher levels in tumors without estrogen and progesterone receptors or human epidermal growth factor receptor-2, compared with receptor-positive tumors (20). Furthermore, *FAM83H*, the paralog of

FAM83B, is overexpressed in androgen independent-prostate cancer (21). These findings could indicate that *FAM83B* has an oncogenic role without aberrant signals from driver gene mutations or overexpressed hormone receptors. *FAM83B* was first reported by Cipriano and colleagues (15) to be correlated with anchorage-independent growth in breast cancer cell lines using a validation-based insertion mutagenesis method. *FAM83B* is a member of the FAM83 family, which includes eight members (*FAM83A* to *H*) characterized by a domain of unknown function 1669 (DUF1669) containing an N terminal phospholipase D-like motif. The function of *FAM83B* remains unclear, however, the mechanism of promote MAPK and PI3K signaling pathway through DUF1669 was proposed (15). *FAM83B* may interfere with the binding of 14-3-3 protein to CRAF, thereby promoting membrane localization of CRAF, and promoting downstream signals to MAPK (15, 22, 23). Furthermore, *FAM83B* may also bind to p85 and p110 subunits of PI3K to promote PI3K/AKT signaling (24), which promotes

oncogenic transformation through phospholipase D activation (25), and shows resistance against EGFR-TKI (15, 23, 26). To determine whether FAM83B promotes cellular proliferation via ERR and/or PI3K/AKT signaling cascades, further study will be required using the corresponding kinase inhibitors.

Our knockdown study of *FAM83B* showed that its expression was associated with tumor proliferation in cell lines expressing high levels of *FAM83B.* H1975 cells showed that knockdown of low levels of *FAM83B* also inhibited proliferation. However, we need to exclude the possibility that FAM83B may affect the cell number in HLC-1 and H1975 cells via modulating cell death. Moreover, the gain of function of FAM83B should be also verified in future experiments.

In normal human tissues, FAM83B is expressed at relatively higher levels in lung, digestive tract, breast, bladder, uterus, and skin (20). Of all the *FAM83* members, only *FAM83H* knockout mice, which live for only 2 weeks, have been reported, and

FAM83H is proposed to play a role in the maintenance of cell homeostasis (21, 27). Other FAM83 family members, including *FAM83B*, may also be required at certain levels, even in normal cells to regulate cell functions.

FAM83 family members are usually associated with poor cancer prognosis (20). Our study of lung ADC also showed that *FAM83B* correlates with poor prognosis; however, our previous study reported high *FAM83B* expression to be a biomarker for good DFS prognosis in lung SqCC (14). Snijders et al. conducted a meta-analysis of several databases (28-30) and suggested that lung ADC expresses relatively high levels of *FAM83A, D, E, F*, and *H*, but *FAM83A, B, D,* and *F* correlate with prognosis. In lung SqCC, all *FAM83* members except *FAM83E* are highly expressed, but only *FAM83A* correlates with poor prognosis (20). These findings indicate *FAM83B* has separate roles among cancers or tumor subtypes.

FAM83 family members, including *FAM83B*, are more highly expressed in

lung cancer than in normal lung tissue, and their expression is reflected in the T factor of TNM classification (28, 31). Our study did not show a correlation between tumor size and *FAM83B* expression. This contradiction was caused by the fact that the T factor includes not only tumor size but pleural invasion. Both tumor size and pleural invasion had no significant effect on *FAM83B* expression.

FAM83B RNAi suppressed proliferation of human lung cancer cell lines. This result indicates that *FAM83B* could be a potential therapeutic target against EGFR-WT malignancies, which account for 47%-88.7% of lung ADC (4, 28) and which are rarely indicated for molecular targeted therapies.

Limitations of this study include lack of evaluation of advanced or recurrent cancer cohorts because the patient cohort was derived from operable lung ADC cases biased to early stages. Moreover, this study did not examine other driver mutations of lung ADC, such as KRAS, ALK fusions. Subdivision based on other genomic or

molecular features could further explain the function of *FAM83B* in lung ADC. Further investigation is required.

Acknowledgements

This research was partially supported by a grant for translational research programs of Fukushima Prefecture. H. Suzuki received research support from Bristol Myers Squibb, AstraZeneca, and Tsumura, outside the submitted work. T. Yamaura received research support from AstraZeneca, outside the submitted work. S. Muto had been employed by AstraZeneca, outside the submitted work. Y. Yanagisawa had been employed by Nippon Gene Co., Ltd., outside the submitted work. R. Honma is employed by Nippon Gene Co., Ltd., outside the submitted work. The remaining authors declare no conflict of interest. The authors thank H I, M Otsuki, E Otomo, and Y Kikuta for their technical supports.

References

1. Stewart BW, Wild CP (ed.): World Cancer Report 2014. Lyon: IARC; 2014.

2. National cancer institute: https://seer.cancer.gov. Accessed 17.10.03.

3. National Comprehensive Cancer Network: https://www.nccn.org/professionals/physician_gls/f_guidelines.asp. Accessed 17.04.03.

4. Kohno T, Tsuta K, Tsuchihara K, Nakaoku T, Yoh K, Goto K: RET fusion gene: translation to personalized lung cancer therapy. Cancer Sci 104: 1396-1400, 2013.

5. Rosell R, Ichinose Y, Taron M, Sarries C, Queralt C, Mendez P, Sanchez JM, Nishiyama K, Moran T, Cirauqui B, et al: Mutations in the tyrosine kinase domain of the EGFR gene associated with gefitinib response in non-small-cell lung cancer. Lung cancer 50: 25-33, 2005.

6. Shaw AT and Solomon B: Targeting anaplastic lymphoma kinase in lung cancer. Clin Cancer Res 17: 2081-6, 2011.

7. Mok TS, Wu YL, Thongprasert S, Yang CH, Chu DT, Saijo N, Sunpaweravong P, Han B, Margono B, Ishinose Y, et al: Gefitinib or carboplatin–paclitaxel in pulmonary adenocarcinoma. N Engl J Med 361: 947-957, 2009.

8. Solomon BJ, Mok T, Kim DW, Wu YL, Nakagawa K, Mekhail T, Felip E, Cappuzzo F, Paolini J, Usari T, et al: First-line crizotinib versus chemotherapy in ALK-positive lung cancer. N Engl J Med 371: 2167-2177, 2014.

9. Borghaei H, Paz-Ares L, Horn L, Spigel DR, Steins M, Ready NE, Chow LQ, Vokes EE, Felip E, Holgado E, et al: Nivolumab versus docetaxel in advanced nonsquamous non-small-cell lung cancer. N Engl J Med 373: 1627-1639, 2015.

10. Patel JD, Socinski MA, Garon EB, Reynolds CH, Spigel DR, Olsen MR, Hermann RC, Jotte RM, Beck T, Richards DA, et al: PointBreak: a randomized phase III study of pemetrexed plus carboplatin and bevacizumab followed by maintenance pemetrexed and bevacizumab versus paclitaxel plus carboplatin and bevacizumab

followed by maintenance bevacizumab in patients with stage IIIB or IV nonsquamous non-small-cell lung cancer. J Clin Oncol 31: 4349-4357, 2013.

11. Park K, Tan EH, O'Byrne K, Zhang L, Boyer M, Mok T, Hirsh V, Yang JC, Lee KH, Lu S, et al: Afatinib versus gefitinib as first-line treatment of patients with EGFR mutation-positive non-small-cell lung cancer (LUX-Lung 7): a phase 2B, open-label, randomised controlled trial. Lancet Oncol 17: 577-589, 2016.

12. Chan BA and Hughes BG: Targeted therapy for non-small cell lung cancer: current standards and the promise of the future. Transl Lung Cancer Res 4: 36-54, 2015.

13. Sholl LM, Aisner DL, Varella-Garcia M, Berry LD, Dias-Santagata D, Wistuba II, Chen H, Fujimoto J, Kugler K, Franklin WA, et al: Multi-institutional oncogenic driver mutation analysis in lung adenocarcinoma: the lung cancer mutation consortium experience. J Thorac Oncol 10: 768-777, 2015.

14. Okabe N, Ezaki J, Yamaura T, Muto S, Osugi J, Tamura H, Imai J, Ito E,

Yanagisawa Y, Honma R, et al: FAM83B is a novel biomarker for diagnosis and prognosis of lung squamous cell carcinoma. Int J Oncol 46: 999-1006, 2015.

15. Cipriano R, Graham J, Miskimen KL, Bryson BL, Bruntz RC, Scott SA, Brown HA, Stark GR, and Jackson MW: FAM83B mediates EGFR- and RAS-driven oncogenic transformation. J Clin Invest 122: 3197-3210, 2012.

16. Miura A, Honma R, Togashi T, Yanagisawa Y, Ito E, Imai J, Goshima N, Watanabe S, and Nomura N: Differential responses of normal human coronary artery endothelial cells against multiple cytokines comparatively assessed by gene expression profiles. FEBS Lett 580: 6871-6879, 2006.

17. Livak KJ, and Schmittgen TD: Analysis of relative gene expression data using real-time quantitative PCR and the 2-ΔΔCT method. Methods 25: 402-408, 2001.

18. Laemmli UK: Cleavage of structural proteins during the assembly of the head of bacteriophage T4. Nature 227: 680-5, 1970.

19. Towbin H, Staehelin T, and Gordon J: Electrophoretic transfer of proteins from polyacrylamide gels to nitrocellulose sheets: procedure and some applications. Proc Natl Acad Sci USA 76: 4350-4, 1979.

20. Snijders AM, Lee SY, Hang B, Hao W, Bissell MJ, and Mao JH: FAM83 family oncogenes are broadly involved in human cancers: an integrative multi-omics approach. Mol Oncol 11: 167-179, 2017.

21. Bartel CA, Parameswaran N, Cipriano R, and Jackson MW: FAM83 proteins: fostering new interactions to drive oncogenic signaling and therapeutic resistance. Oncotarget 7: 52597-52612, 2016.

22. Tzivion G, Luo Z, and Avruch J: A dimeric 14-3-3 protein is an essential cofactor for Raf kinase activity. Nature 394: 88-92, 1998.

23. Cipriano R, Miskimen KL, Bryson BL, Foy CR, Bartel CA, and Jackson MW: Conserved oncogenic behavior of the FAM83 family regulates MAPK signaling in

human cancer. Mol Cancer Res 12: 1156-1165, 2014.

24. Cipriano R, Miskimen KL, Bryson BL, Foy CR, Bartel CA, and Jackson MW: FAM83B-mediated activation of PI3K/AKT and MAPK signaling cooperates to promote epithelial cell transformation and resistance to targeted therapies. Oncotarget 4: 729-738, 2013.

25. Cipriano R, Bryson BL, Miskimen KL, Bartel CA, Hernandez-Sanchez W, Bruntz RC, Scott SA, Lindsley CW, Brown HA, and Jackson MW: Hyperactivation of EGFR and downstream effector phospholipase D1 by oncogenic FAM83B. Oncogene 33: 3298-3306, 2014.

26. Grant S: FAM83A and FAM83B: candidate oncogenes and TKI resistance mediators. J Clin Invest 122: 3048-3051, 2012.

27. Wang SK, Hu Y, Yang J, Smith CE, Richardson AS, Yamakoshi Y, Lee YL, Seymen F, Koruyucu M, Gencay K, et al: Fam83h null mice support a neomorphic

mechanism for human ADHCAI. Mol Genet Genomic Med 4: 46-47, 2016.

28. The Cancer Genome Atlas Research Network: Comprehensive molecular profiling of lung adenocarcinoma. Nature 511: 543-550, 2014.

29. Carithers LJ and Moore HM: The genotype-tissue expression (GTEx) project. Biopreserv Biobank 13: 307-308, 2015.

30. Mele M, Ferreira PG, Reverter F, DeLuca DS, Monlong J, Sammeth M, Young TR, Goldmann JM, Pervouchine DD, Sullivan TJ, et al: Human genomics. The human transcriptome across tissues and individuals. Science 348: 660-665, 2015.

31. Rhodes DR, Kalyana-Sundaram S, Mahavisno V, Varambally R, Yu J, Briggs BB, Barrette TR, Anstet MJ, Kincead-Beal C, Kulkami P, et al: Oncomine 3.0: genes, pathways, and networks in a collection of 18,000 cancer gene expression profiles. Neoplasia 9: 166-180, 2007.

Figure legends

Figure 1. Expression levels of *FAM83B* obtained by cDNA microarray analysis of tumors stratified by the presence or absence of *EGFR* mutation, and adjacent normal tissue. The expression of *FAM83B* in tumors with wild-type *EGFR* was significantly higher compared with tumors with mutant EGFR ($p < 0.001$) or adjacent normal tissue ($p < 0.001$). No significant difference in *FAM83B* expression was found between tumors with mutant EGFR and adjacent normal tissue ($p = 0.852$). Horizontal bars represent mean expression levels. NOTE; EGFR; epidermal growth factor receptor, FAM83B; family with sequence similarity 83, member B, Mut; mutant, Normal; normal adjacent lung tissue, WT; wild type.

Figure 2. Kaplan–Meier curves showing patient survival after lung resection.

(A) Disease-free survival (DFS) and (B) overall survival (OS) of all eligible participants.

(C,D) DFS and OS of the patients stratified by tumors with wild-type epidermal growth factor receptor.

Figure 3. The effect of *FAM83B* on the proliferation of lung cancer cell lines. (A, B) *FAM83B* mRNA and protein levels were examined by qRT-PCR and western blotting, respectively, in MCF7, H1975, H2347, and HLC1 cells. The Rq ratios to MCF7 cells were; H1975: 0.0061, H2347: 2.2103, and HLC1: 7.1968. (C-H) RNAi was performed in HLC-1 and H1975 cells. Depletion of *FAM83B* mRNA and protein was confirmed by qRT-PCR (C and F) and western blotting (D and G), respectively. Rq ratios to negative control were; HLC-1: 0.3519 and H1975: 0.1675 for qRT-PCR. (E and H) Cell proliferation assay in HLC-1 and H1975 cells after RNAi. Cell numbers were counted over time. Cell growth was significantly suppressed in HLC-1 and H1975 cells. (E and H) Original magnification x40. NOTE; FAM83B; family with sequence similarity 83, member B, Rq ratio: relative quantification ratio, **: $p < 0.01$, *: $p < 0.05$, N/C: negative control.

Figure 4. *FAM83B* siRNA transfection efficiency and RNA interference in cultured

cells. (A-D) Transfection of *FAM83B* siRNA significantly suppressed cell growth of MCF7, HLC-1, and H1975 cells but not of H2347 cells. (E) qRT-PCR showed that both siRNA-8 and siRNA-9 reduced the expression of *FAM83B*. (F) Immunoblotting analysis showed that FAM83B signals were significantly depleted in MCF7 cells transfected with siRNA-8 or siRNA-9. (G) Both siRNA-8 and siRNA-9 suppressed cell growth, especially siRNA-9. NOTE; Rq: quantification relative to negative control, **: $p < 0.01$, *: $p < 0.05$, P/C: positive control, N/C: negative control.

TABLE I. Clinicopathological and Genetic Features of Lung Adenocarcinoma Patients According to FAM83B Expression in Tumor Tissue

		FAM83B Expression		
Variables		**High (n=55)**	**Low (n=161)**	**p-value**
Age	≦69 years old	25 (45.5%)	87 (54.0%)	0.271
	≧70 years old	30 (54.5%)	74 (46.0%)	
Sex	Male	39 (70.9%)	80 (49.7%)	0.006
	Female	16 (29.1%)	81 (50.3%)	
Smoking history	Never smoker	18 (32.7%)	87 (54.0%)	0.006
	Former or Current smoker	37 (67.3%)	74 (46.0%)	
EGFR gene	Wild-type	43 (78.2%)	75 (46.6%)	＜0.001

	Mutant	12 (21.8%)	86 (53.4%)	
Pathological subtype[a]	Lepidic	9 (16.4%)	36 (22.4%)	＜0.001
	Papillary	27 (49.1%)	99 (61.5%)	
	Acinar	5 (9.1%)	12 (7.5%)	
	Solid	7 (12.7%)	10 (6.2%)	
	Other variants	7 (12.7%)	4 (2.4%)	
Tumor size	≦ 3cm	29 (52.7%)	102 (63.4%)	0.164
	>3 cm	26 (47.3%)	59 (36.6%)	
LN metastasis	N0	46 (83.6%)	131 (81.4%)	0.706
	N1/N2/N3	9 (16.4%)	30 (18.6%)	
Distant metastasis	M0	54 (98.2%)	159 (98.8%)	1.000

	M1	1 (1.8%)	2 (1.2%)	
Pleural invasion	(-)	39 (70.9%)	120 (74.5%)	0.598
	(+)	16 (29.1%)	39 (24.2%)	
Lymphatic invasion	(-)	44 (80.0%)	114 (70.8%)	0.184
	(+)	11 (20.0%)	47(29.2%)	
Vascular invasion	(-)	37 (67.3%)	122 (75.7%)	0.217
	(+)	18 (32.7%)	39 (24.2%)	

FAM83B; family with sequence similarity 83, member B, EGFR; epidermal growth factor receptor, LN; lymph node. NOTE: [a]IASLC/ATS/ERS adenocarcinoma classification.

TABLE II. Correlation between Clinicopathological Characteristics of Lung Adenocarcinoma Patients and FAM83B Expression in Tumors

Variables	Odds ratio	95% Confidence Interval	p-value
Univariate analysis			
≧70 years old	1.411	0.763–2.609	0.272
Male	2.468	1.277–4.769	0.007
Smoking	2.417	1.271–4.596	0.007
Wild-type *EGFR*	0.243	0.120–0.495	<0.001
Histological Subtype[a]	2.202	0.795–6.101	0.129
Tumor size>3cm	1.550	0.835–2.878	0.165
LN metastasis	0.854	0.377–1.934	0.706
Distant metastasis	1.472	0.131–16.560	0.754
Pleural invasion	1.201	0.607–2.373	0.599
Lymphatic invasion	0.606	0.288–1.275	0.187
Vascular invasion	1.522	0.780–2.970	0.218
Multivariate analysis			
Wild-type *EGFR*	0.243	0.120–0.495	<0.001

NOTE: [a]Comparison between predominantly non-solid and solid histological subtypes
EGFR; epidermal growth factor receptor, FAM83B; family with sequence similarity 83, member B.

TABLE III. Univariate and Multivariate Predictors of Disease-Free Survival and Overall Survival

Variables	Unfavorable/Favorable	Hazard ratio (95% Confidence Interval)	p-value
DFS			
Univariate analysis			
FAM83B	High/low	2.415(1.195–4.881)	0.014
Age	≧70/<70	1.183 (0.604–2.318)	0.624
Sex	Male/female	2.502 (1.196–5.233)	0.015
EGFR gene	Wild-type/mutant	0.595 (0.298–1.189)	0.142
Pack-year	>5/≦5	1.455 (0.735–2.881)	0.282
Tumor size	>3cm/≦3cm	1.073 (0.537–2.142)	0.843
N[a]	N1+N2+N3/N0	3.852 (1.867–7.948)	<0.001
pl[b]	Positive/negative	2.599 (1.299–5.197)	0.007
ly[c]	Positive/negative	2.347 (1.173–4.696)	0.016
v[d]	Positive/negative	2.929 (1.477–5.811)	0.002
Multivariate analysis			
FAM83B	High/low	2.286 (1.129–4.631)	0.022
N[a]	N1+N2+N3/N0	3.699 (1.788–7.655)	<0.001

OS			
Univariate analysis			
FAM83B	High/low	3.814 (1.619–8.989)	0.002
Age	≧70/<70	1.010 (0.429–2.380)	0.981
Sex	Male/female	3.241 (1.187–8.854)	0.022
EGFR gene	Wild-type/mutant	0.297 (0.108–0.813)	0.018
Pack-year	>5/≦5	2.080 (0.839–5.154)	0.114
Tumor size	>3cm/≦3cm	1.297 (0.547–3.079)	0.555
N[a]	N1+N2+N3/N0	4.342 (1.798–10.483)	0.001
pl[b]	Positive/negative	5.313 (2.234–12.634)	<0.001
ly[c]	Positive/negative	2.577 (1.085–6.117)	0.032
v[d]	Positive/negative	3.338 (1.414–7.877)	0.006
Multivariate analysis			
FAM83B	High/low	3.723 (1.568–8.842)	0.003
pl[b]	Positive/negative	5.098 (2.119–12.264)	<0.001
v[d]	Positive/negative	2.529 (1.066–6.001)	0.035

NOTE: [a]Lymph node metastasis according to Union for International Cancer Control 7th edition, [b]pleural invasion, [c]lymphovascular invasion, and [d]vascular invasion.

DFS; disease-free survival, EGFR; epidermal growth factor receptor, FAM83B; family

with sequence similarity 83, member B, N; nodes, OS; overall survival

Figure 1

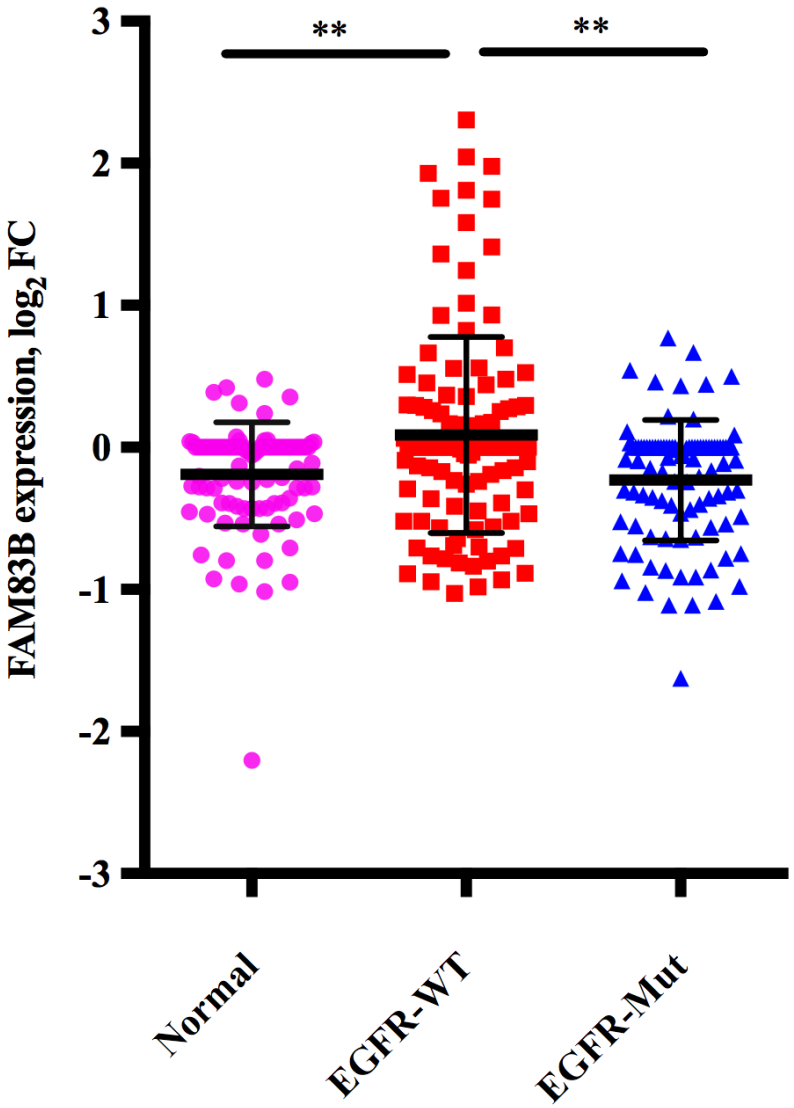

Figure 2

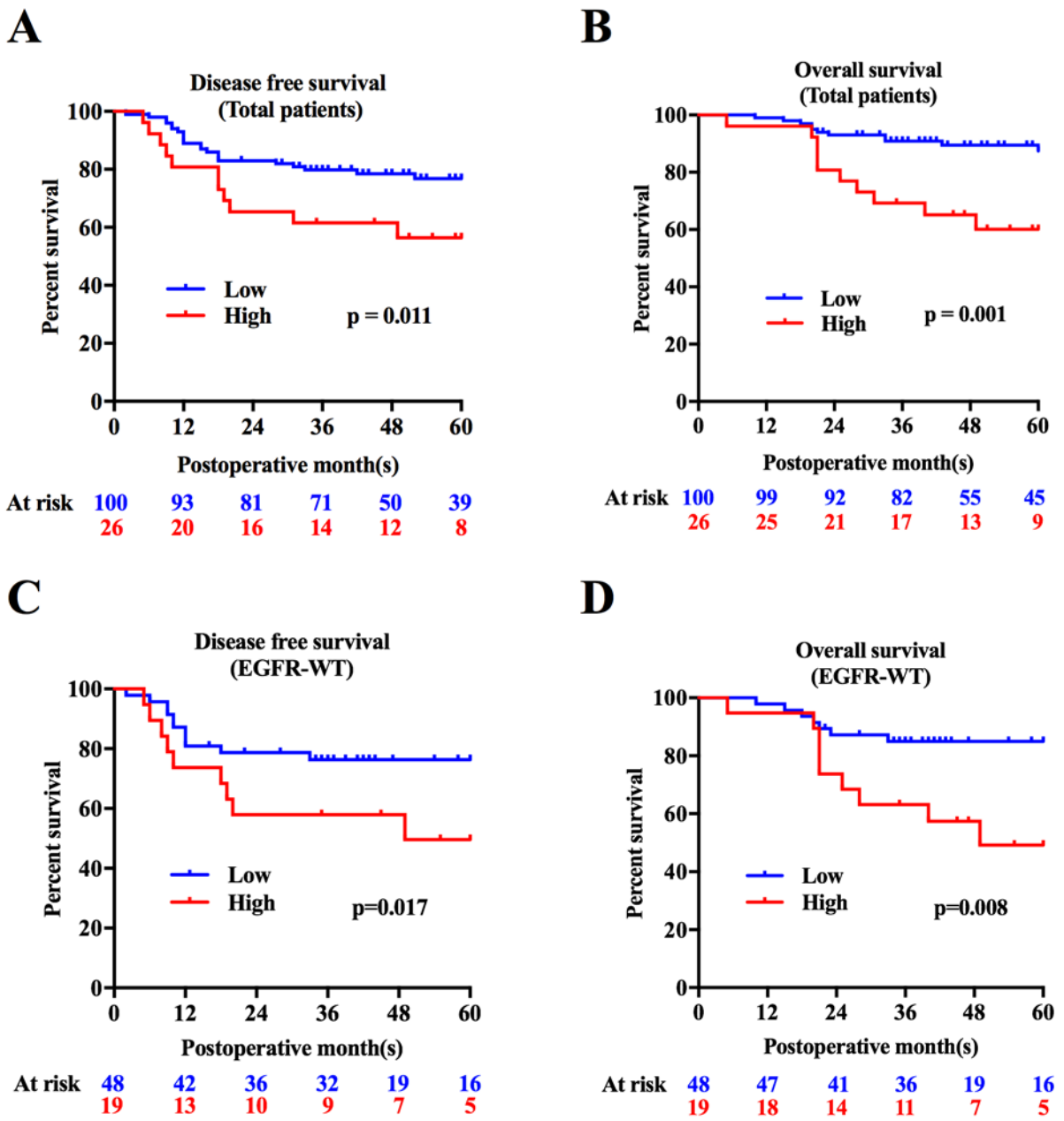
A
Disease free survival
(Total patients)
Percent survival
100
80
60
40
20
0
Low
High
p = 0.011
0
12
24
36
48
60
Postoperative month(s)
At risk 100 93 81 71 50 39
26 20 16 14 12 8
B
Overall survival
(Total patients)
Percent survival
Low
High
p = 0.001
Postoperative month(s)
At risk 100 99 92 82 55 45
26 25 21 17 13 9
C
Disease free survival
(EGFR-WT)
Percent survival
Low
High
p=0.017
Postoperative month(s)
At risk 48 42 36 32 19 16
19 13 10 9 7 5
D
Overall survival
(EGFR-WT)
Percent survival
Low
High
p=0.008
Postoperative month(s)
At risk 48 47 41 36 19 16
19 18 14 11 7 5

Figure 3

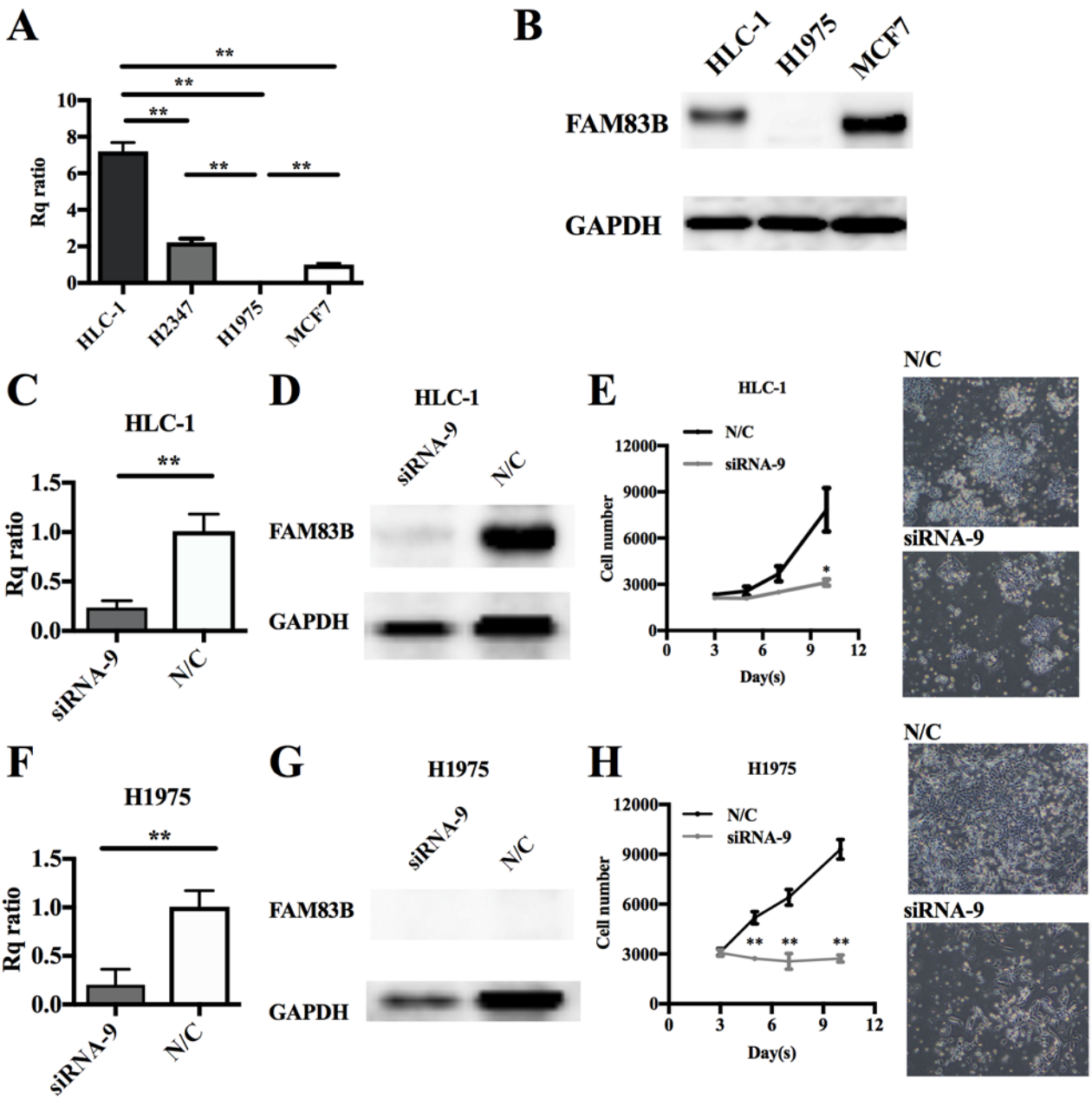
A
**
**
**
**
**
Rq ratio
10
8
6
4
2
0
HLC-1
H2347
H1975
MCF7
B
HLC-1
H1975
MCF7
FAM83B
GAPDH
C
HLC-1
**
Rq ratio
1.5
1.0
0.5
0.0
siRNA-9
N/C
D
HLC-1
siRNA-9
N/C
FAM83B
GAPDH
E
HLC-1
N/C
siRNA-9
Cell number
12000
9000
6000
3000
0
0
3
6
9
12
Day(s)
*
N/C
siRNA-9
F
H1975
**
Rq ratio
1.5
1.0
0.5
0.0
siRNA-9
N/C
G
H1975
siRNA-9
N/C
FAM83B
GAPDH
H
H1975
N/C
siRNA-9
Cell number
12000
9000
6000
3000
0
0
3
6
9
12
Day(s)
**
**
**
N/C
siRNA-9

Figure 4

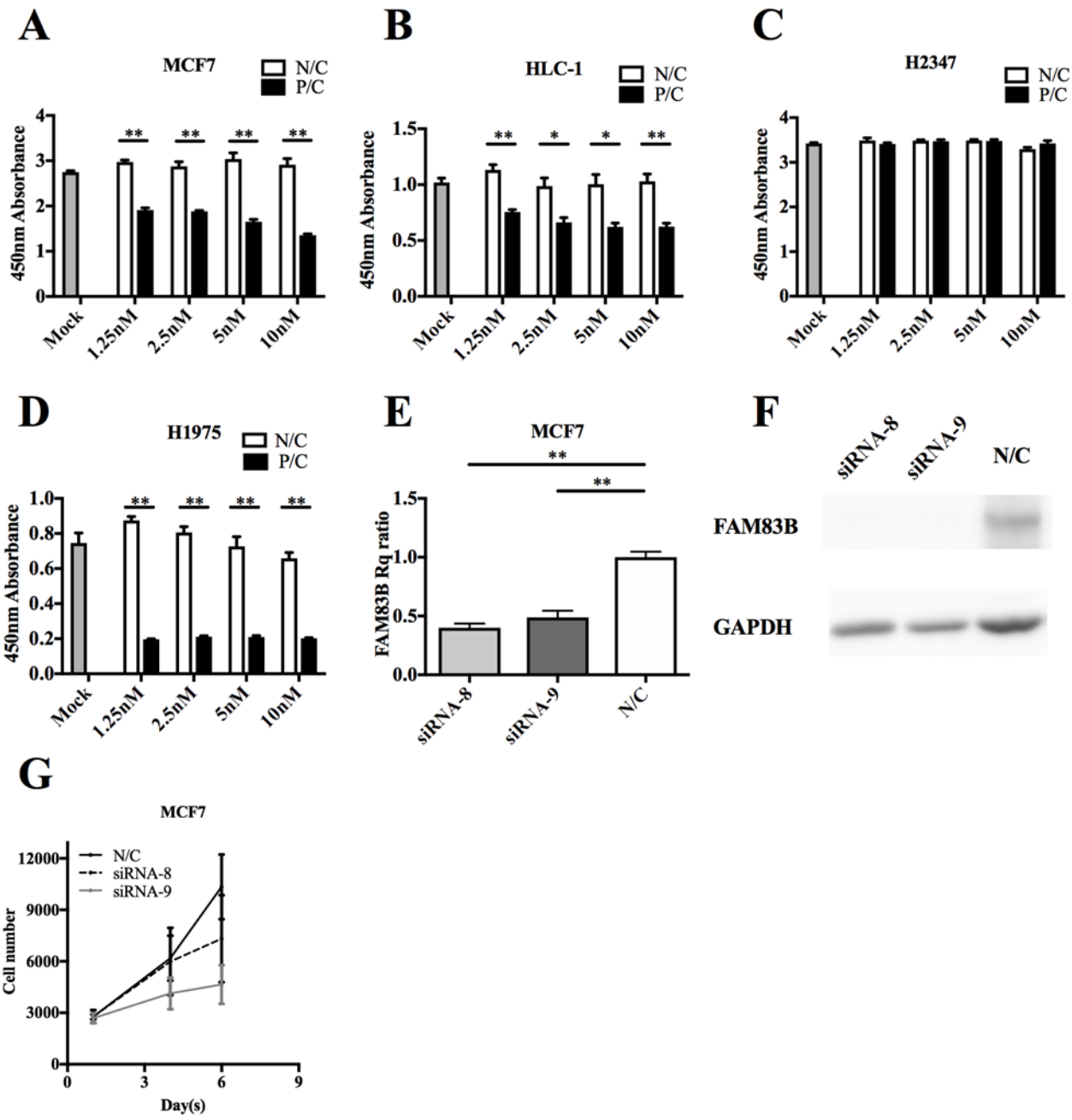
A
MCF7
N/C
P/C
450nm Absorbance
Mock
1.25nM
2.5nM
5nM
10nM
B
HLC-1
C
H2347
D
H1975
E
MCF7
FAM83B Rq ratio
siRNA-8
siRNA-9
N/C
F
siRNA-8
siRNA-9
N/C
FAM83B
GAPDH
G
MCF7
N/C
siRNA-8
siRNA-9
Cell number
Day(s)